Structural transition in interdependent networks with regular interconnections

Article *in* PHYSICAL REVIEW E · January 2019

DOI: 10.1103/PhysRevE.99.012311

Xiangrong Wang
Delft University of Technology

Yamir Moreno
University of Zaragoza

Structural transition in interdependent networks with regular interconnections

Xiangrong Wang,[1,*] Robert E. Kooij,[1,2] Yamir Moreno,[3,4,5] and Piet Van Mieghem[1]
[1]*Faculty of Electrical Engineering, Mathematics and Computer Science, Delft University of Technology, Delft, The Netherlands*
[2]*iTrust Centre for Research in Cyber Security, Singapore University of Technology and Design, Singapore*
[3]*Institute for Biocomputation and Physics of Complex Systems (BIFI), University of Zaragoza, Zaragoza 50009, Spain*
[4]*Department of Theoretical Physics, University of Zaragoza, Zaragoza 50009, Spain*
[5]*ISI Foundation, Turin, Italy*

(Received 31 July 2018; revised manuscript received 19 December 2018; published 7 January 2019)

Networks are often made up of several layers that exhibit diverse degrees of interdependencies. An interdependent network consists of a set of graphs G that are interconnected through a weighted interconnection matrix B, where the weight of each intergraph link is a non-negative real number p. Various dynamical processes, such as synchronization, cascading failures in power grids, and diffusion processes, are described by the Laplacian matrix Q characterizing the whole system. For the case in which the multilayer graph is a multiplex, where the number of nodes in each layer is the same and the interconnection matrix $B = pI$, I being the identity matrix, it has been shown that there exists a structural transition at some critical coupling p^*. This transition is such that dynamical processes are separated into two regimes: if $p > p^*$, the network acts as a whole; whereas when $p < p^*$, the network operates as if the graphs encoding the layers were isolated. In this paper, we extend and generalize the structural transition threshold p^* to a regular interconnection matrix B (constant row and column sum). Specifically, we provide upper and lower bounds for the transition threshold p^* in interdependent networks with a regular interconnection matrix B and derive the exact transition threshold for special scenarios using the formalism of quotient graphs. Additionally, we discuss the physical meaning of the transition threshold p^* in terms of the minimum cut and show, through a counterexample, that the structural transition does not always exist. Our results are one step forward on the characterization of more realistic multilayer networks and might be relevant for systems that deviate from the topological constraints imposed by multiplex networks.

DOI: 10.1103/PhysRevE.99.012311

I. INTRODUCTION

An interdependent network, also called an interconnected network or a network of networks, is a multilayer network consisting of different types of networks that depend upon each other for their functioning [1]. The most illustrative example of these systems is perhaps given by multilayer power networks, in which the power system is represented in one layer which in turn is connected to a communication network whose topology is encoded by another layer. The nodes in the former are controlled by those in the second, whereas at the same time the elements of the communication layer need power to function [2], closing the feedback between the two graphs. The study of the structure and dynamics of interdependent networks is of utmost importance, as critical infrastructures such as the previous one, and other telecommunications, transportation, water-, oil-, and gas-supply systems, etc., are highly interconnected and mutually depend upon each other. As for the dynamics, the framework of multilayer interdependent networks constitutes a useful approach to address catastrophic events such as large-scale blackouts, whose causes are rooted in the inherent vulnerability associated to the interdependencies between the different components of a complex multilayer system: the failure of one infrastructure propagates to another infrastructure [3] and so on. Indeed, Little [4] has proposed to view critical infrastructures as systems of systems so as to understand their robustness against cascading failures.

A key aspect of multilayer networks that has received less attention is the coupling between the layers that make up the whole system, as it can modify the outcome of dynamical processes that run on top of them. For example, Buldyrev *et al.* [5] showed that the collapse of interdependent networks occurs abruptly while the failure of individual networks is approached continuously. Also, the epidemic threshold for disease spreading processes is characterized by both the topology of each coupled network and the interconnection between them [6–9]. On the other hand, the authors of [10] studied an interdependent model consisting of two connected networks, G_1 and G_2, with weighted interconnection links. The coupling weight between the two networks is determined by a non-negative real value p, which, for instance, can be interpreted as the power dispatched by an element of the power layer in the power-communication system above. The previous interdependent system has been shown [10,11] to exhibit a structural transition that takes place at a coupling value, p^*, that separates two regimes: for $p > p^*$, the interdependent network acts as a whole, whereas for $p < p^*$, the network is structurally separated and the layers G_1 and G_2 behave as if they were isolated. The explicit expression for the transition threshold p^* is determined in [12]. Rapisardi *et al.* [13] study the algebraic connectivity of interdependent networks using a perturbation approach. Their study reveals multiple structural

*x.wang-2@tudelft.nl

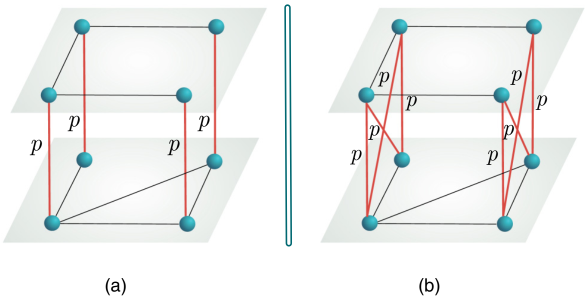

FIG. 1. The figure depicts two interdependent networks that only differ in their interlayer couplings: the left panel represents the case studied in [10], which is however not commonly found in real systems as it constrains all interlayer couplings to follow a one-to-one interconnection pattern. On the contrary, the right panel represents a scenario in which the interlayer connectivity follows a k-to-k coupling scheme, and although still not fully realistic given the regularity—i.e., homogeneity—of the interconnection pattern, it is more complex and representative of real interdependent networks. (a) one-to-one interconnection and (b) k-to-k interconnection (here $k = 2$).

transitions, where each single layer dominates the dynamics on the whole system.

The model in [10] focuses on a one-to-one interconnection between nodes of different layers. This means that one node in graph G_1 connects to one and only one node in graph G_2 and vice versa. When the interconnection pattern is not one to one, as in most real-world examples, the determination of the transition threshold p^* is more complex. Examples of a multiple-to-multiple interconnection pattern can be found in (i) smart grids consisting of coupled sensor networks and power networks [14–16] where a sensor might control multiple power stations due to cost and energy constraints; (ii) functional brain networks modeled as multilayer networks where one brain region in one layer might be functionally connected to any node in another layer [17]; and (iii) infrastructures like power networks and fiber-optic communication systems that are geographically interconnected based on spatial proximity [18,19]. Given the abundance of the previous examples and similar scenarios, it is thus relevant to extend the study of structural transitions to such cases.

In this paper, we investigate the structural threshold p^* of interdependent networks with a general k-to-k (k is a positive integer) interconnection; see Fig. 1 and Sec. II, where we introduce these networks. In Sec. III, we derive upper and lower bounds for the structural threshold p^* and report on certain topologies whose exact transition threshold can be calculated from its quotient graph. The physical interpretation of the structural threshold p^* with respect to the minimum cut is presented in Sec. IV. Next, in Sec. V, we derive the exact structural threshold p^* for special cases of interconnectivity and present a counterexample for the nonexistence of the structural threshold p^*. Section VI concludes the paper.

II. INTERDEPENDENT NETWORKS

Let the graph $G(N, L)$ represent an interdependent, multilayer network consisting of two layers (networks), described by graph G_1 with n nodes and graph G_2 with m nodes. The total number of nodes in G is thus $N = n + m$. An interdependent link connects a node i in network G_1 to a node j in network G_2. Within this paper, we use mainly the terminology of interdependent networks or multilayer networks. The relations and the differences between terminology, like multiplex networks, interacting networks, and interconnected networks, are reviewed in [20, Table 1]. The adjacency matrix A of the interdependent network G has a block structure of the form

$$A = \begin{bmatrix} (A_1)_{n\times n} & B_{n\times m} \\ (B^T)_{m\times n} & (A_2)_{m\times m} \end{bmatrix},$$

where A_1 is the $n \times n$ adjacency matrix of G_1, A_2 is the $m \times m$ adjacency matrix of G_2, and B is the $n \times m$ coupling or interconnection matrix encoding the connections between G_1 and G_2. If each interdependent link is weighted with a nonnegative real number p, the matrix B is a weighted matrix with elements $b_{ij} = p$ if node i in G_1 connects to node j in G_2, otherwise $b_{ij} = 0$. Note that the definition for B used in [1] is more general, as the weights of each interdependent link can be different. Here, the matrix B corresponds to a scenario in which each interdependent link has a weight p, the same for all links of this kind.

A *k-to-k interconnection*, where $k = 1, 2, \dots, \min(n, m)$, means that one node in graph G_1 connects to k nodes in graph G_2 and vice versa. We only consider undirected interconnection links. The k-to-k interconnection requires a square matrix B with $n = m$, because the number kn of interconnection links computed in graph G_1 must be equal to the number km computed in graph G_2, i.e., $kn = km$. For the rest of this article, we focus on a square interconnection matrix B with $n = m$ and the subscript of matrix B is omitted. Furthermore, as noted before, the k-to-k interconnectivity pattern is a generalization of the one-to-one scheme ($B = pI$) studied in [5,10,12].

For a square coupling matrix B, a k-to-k interconnection can be constructed via a circulant matrix [21] with the form

$$B = \begin{bmatrix} c_1 & c_2 & c_3 & \cdots & c_n \\ c_n & c_1 & c_2 & \cdots & c_{n-1} \\ c_{n-1} & c_n & c_1 & \cdots & c_{n-2} \\ \vdots & \vdots & \vdots & \ddots & \vdots \\ c_2 & c_3 & c_4 & \cdots & c_1 \end{bmatrix}, \quad (1)$$

where the row vector $(c_1, c_2, \dots, c_n)$ has exactly k elements equal to p and $n - k$ elements that are 0. A circulant matrix is a matrix where each row is the same as the previous one, but the elements are shifted one position to the right and wrapped around at the end. Circulant topology is commonly used to represent the periodic and discrete filters in the field of discrete signal processing [22]. The circulant representation enables filtering the input signals by using matrix-vector multiplication and outputting the linear combinations of the input signals. The circulant representation enables filtering the input signals by using matrix-vector multiplication and outputting the linear combinations of the input signals. The circulant interconnection topology is commonly used in core telecommunication networks. Such networks often consist of a primary network and a back-up network. Each node in the primary core is typically connected to two nodes in the back-up network, for the sake of redundancy. The resulting interconnection topology is circulant. Circulant matrices are commutative [23]. For example, a symmetric matrix B for a 2-to-2 ($k = 2$) interconnection can be written as

$$B = \begin{bmatrix} 0 & p & 0 & \cdots & p \\ p & 0 & p & \cdots & 0 \\ 0 & p & 0 & \cdots & 0 \\ \vdots & \vdots & \vdots & \ddots & \vdots \\ p & 0 & 0 & \cdots & 0 \end{bmatrix}.$$

Analogous to the definition of the Laplacian matrix $Q = \Delta - A$ in a single network, where Δ is the diagonal matrix of node degrees, we use the following diagonal matrices:

$$\Delta_1 \overset{\text{def}}{=} \text{diag}(Bu), \quad \Delta_2 \overset{\text{def}}{=} \text{diag}(B^T u)$$

to define the Laplacian matrix Q of the interdependent network G as

$$Q = \begin{bmatrix} Q_1 + \Delta_1 & -B \\ -B^T & Q_2 + \Delta_2 \end{bmatrix},$$

where Q_1 and Q_2 are the Laplacian matrices of networks G_1 and G_2, respectively. The all-one vector is denoted by u and the subscript of u is used if the dimension is not clear. Since the Laplacian matrix Q is symmetric, the eigenvalues of Q are non-negative and at least one is zero [21]. We order the eigenvalues of the Laplacian matrix Q as $0 = \mu_N \leqslant \mu_{N-1} \leqslant \cdots \leqslant \mu_1$ and denote the eigenvector corresponding to the j-largest eigenvalue by x_j. The second smallest eigenvalue of the Laplacian matrix Q was coined by Fiedler [24] as the algebraic connectivity μ_{N-1} of a graph G. The algebraic connectivity plays a key role in different aspects related to the structure and dynamics of networks, such as in diffusion processes [11,25], synchronization stability [26], and network robustness against failures [27].

The Laplacian eigenvalue equation for the eigenvector $x_k = (x_1^T,\ x_2^T)^T$, where x_1 and x_2 are $n \times 1$ vectors, associated to the eigenvalue μ_k is

$$\begin{bmatrix} Q_1 + \Delta_1 & -B \\ -B^T & Q_2 + \Delta_2 \end{bmatrix} \begin{bmatrix} x_1 \\ x_2 \end{bmatrix} = \mu_k \begin{bmatrix} x_1 \\ x_2 \end{bmatrix}. \tag{2}$$

The normalized vector $x_N = \frac{1}{\sqrt{N}}(u_n^T,\ u_n^T)^T$ is an eigenvector associated to the smallest eigenvalue $\mu_N = 0$ of the Laplacian Q. We briefly present a theorem (in [1, Theorem 3]) to introduce a nontrivial eigenvalue and eigenvector of the Laplacian Q.

Theorem 1. Only if the $n \times m$ interconnection matrix $\widetilde{B}$ has a constant row sum equal to $\frac{\mu^*}{N}m$ and a constant column sum equal to $\frac{\mu^*}{N}n$, which we call the regularity condition for $\widetilde{B}_{n\times m}$,

$$\widetilde{B}u_m = \frac{\mu^*}{N}mu_n$$
$$\widetilde{B}^T u_n = \frac{\mu^*}{N}nu_m$$

then

$$x = \frac{1}{\sqrt{N}}\left[\sqrt{\frac{m}{n}}u_n^T,\ -\sqrt{\frac{n}{m}}u_m^T\right]^T$$

is an eigenvector of Q associated to the eigenvalue

$$\mu^* = \left(\frac{1}{n} + \frac{1}{m}\right)u_n^T \widetilde{B}_{n\times m} u_m$$

and $u_n^T \widetilde{B}_{n\times m} u_m$ equals the sum of the elements in $\widetilde{B}$, representing the total strength of the interconnection between graphs G_1 and G_2.

Corollary 1. Consider an interdependent graph G with N nodes consisting of two graphs each with n nodes, whose interconnections are described by a weighted interconnection matrix B. For a k-to-k interconnection pattern with the coupling weight p on each interconnection link, the vector

$$x = \frac{1}{\sqrt{N}}[u_n^T,\ -u_n^T]^T \tag{3}$$

is an eigenvector of the Laplacian matrix Q of graph G associated to the eigenvalue

$$\mu^* = 2kp. \tag{4}$$

Proof. For a k-to-k interconnection, the row and column sum of the interconnection matrix B is a constant equal to kp,

$$Bu_n = kpu_n, \quad B^T u_n = kpu_n,$$

which obeys the regularity condition in Theorem 1. With $n = m$ and the total coupling strength $u_n^T \widetilde{B}_{n\times m} u_m = kpn$ in Theorem 1, we establish Corollary 1. ■

Corollary 1 shows the existence of an eigenvalue $\mu^* = 2kp$. When graphs G_1 and G_2 are connected and the coupling weight $p \to 0$, the eigenvalue $\mu^* \to 0$ and all the other $N - 2$ eigenvalues (excluding eigenvalues zero and μ^*) approach $x_1^T Q_1 x_1 + x_2^T Q_2 x_2 > 0$. Therefore, for p sufficiently small, the eigenvalue $\mu^* = 2kp$ can be made the smallest positive eigenvalue, which then equals the algebraic connectivity μ_{N-1} of the whole interdependent network G. By increasing the coupling weight p, at some point, the nontrivial eigenvalue $\mu^* = 2kp$ no longer is the second smallest eigenvalue. Hence, there exists a transition threshold p^* such that $\mu_{N-1} \neq 2kp$ when $p > p^*$. Because the eigenvalues of the Laplacian Q are continuous functions of the coupling weight p, the second and third smallest eigenvalues coincide [12] at the point of the transition threshold p^*.

Finally, the Laplacian matrix Q for a k-to-k interconnection can be written as the sum of two matrices,

$$Q = \begin{bmatrix} Q_1 & O \\ O & Q_2 \end{bmatrix} + \begin{bmatrix} kpI & -B \\ -B^T & kpI \end{bmatrix}.$$

Moreover, according to the interlacing theorem for the sum of two matrices [21], a lower bound for the third smallest eigenvalue μ_{N-2} of the Laplacian matrix Q follows

$$\mu_{N-2}(Q) \geqslant \min(\mu_{n-2}(Q_1),\ \mu_{n-2}(Q_2)), \tag{5}$$

where $\mu_{n-2}(Q_1)$ and $\mu_{n-2}(Q_2)$ are the third smallest eigenvalue of graphs G_1 and G_2, respectively.

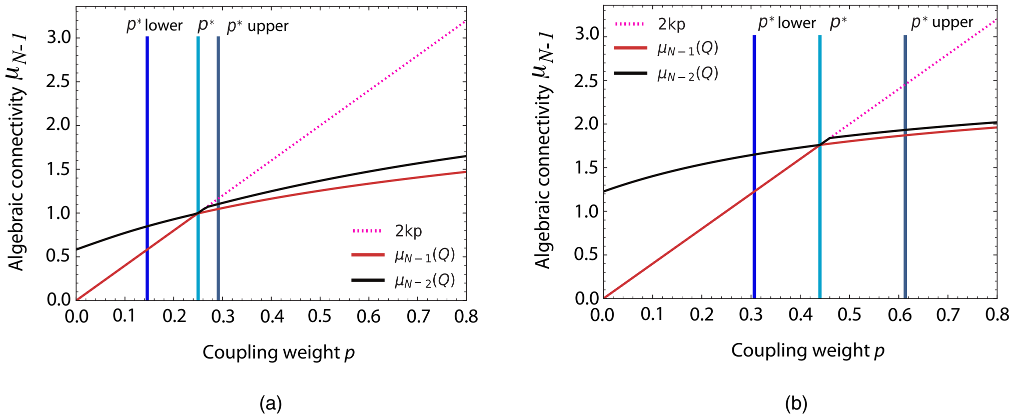

FIG. 2. Accuracy of the upper and lower bounds for the transition threshold p^* in interdependent networks consisting of (a) two Erdős-Rényi graphs and (b) two Barabási-Albert graphs with $n = 500$ and average degree $d_{av} = 6$. The interconnection pattern is a 2-to-2 scheme, i.e., $k = 2$.

III. BOUNDS AND EXACT EXPRESSION FOR THE TRANSITION THRESHOLD p^*

This section derives both upper and lower bounds for the transition threshold p^* of interdependent networks with k-to-k ($k \geqslant 1$) interconnection patterns. We find topologies of interdependent networks where an exact analytical expression for the transition threshold can be attained.

A. Upper and lower bounds for p^*

For a given interconnection matrix B with a k-to-k interconnection, i.e., $Bu = B^T u = kpu$, the Laplacian matrix Q can be written as

$$Q = \begin{bmatrix} Q_1 + kpI & -B \\ -B^T & Q_2 + kpI \end{bmatrix}. \tag{6}$$

For any normalized vector $x = (x_1^T,\ x_2^T)^T$, the quadratic form $x^T Qx$ of the Laplacian Q follows

$$x^T Qx = kp + x_1^T Q_1 x_1 + x_2^T Q_2 x_2 - 2x_1^T B x_2. \tag{7}$$

Let x_1 be an eigenvector associated to the second smallest eigenvalue $\mu_{n-1}(Q_1)$ of Q_1 and $x_2 = 0$. For the vector $x = (x_1^T,\ 0)^T$, its normalization reads $x^T x = x_1^T x_1 = 1$. Thus, the quadratic form in (7) follows $x^T Qx = kp + \mu_{n-1}(Q_1)$. Analogously, we have $x^T Qx = kp + \mu_{n-1}(Q_2)$ when $x_1 = 0$ and x_2 is the eigenvector associated to $\mu_{n-1}(Q_2)$. Applying the Rayleigh inequality [21] to the algebraic connectivity μ_{N-1} yields

$$\mu_{N-1} \leqslant \frac{x^T Qx}{x^T x}.$$

With $x = (x_1^T,\ 0)^T$ or $x = (0,\ x_2^T)^T$, we arrive at

$$\mu_{N-1} \leqslant \min(\mu_{n-1}(Q_1),\ \mu_{n-1}(Q_2)) + kp. \tag{8}$$

The previous equality holds when x is the eigenvector associated to the algebraic connectivity μ_{N-1}.

Next, note that the nontrivial eigenvalue $\mu^* = 2kp$ in (4) corresponding to the eigenvector $x = \frac{1}{\sqrt{N}}(u_n^T,\ -u_n^T)^T$ is no longer the algebraic connectivity μ_{N-1} when $p > p^*$. At the transition threshold p^* the algebraic connectivity is $\mu_{N-1} = 2kp^*$. Substituting $\mu_{N-1} = 2kp^*$ and $p = p^*$ in (8), we arrive at an upper bound for the transition threshold p^*,

$$p^* \leqslant \frac{1}{k} \min(\mu_{n-1}(Q_1),\ \mu_{n-1}(Q_2)). \tag{9}$$

To obtain a lower bound, we apply the min-max theorem to the quadratic term $x_1^T B x_2$ in (7), which yields

$$x_1^T B x_2 \leqslant \sigma_1 x_1^T x_2,$$

where σ_1 is the largest singular value of the matrix B which equals the square root of the largest eigenvalue of the matrix $B^T B$, which equals kp. According to the Cauchy-Schwarz inequality, we have that $x_1^T x_2 \leqslant ||x_1|| ||x_2|| \leqslant \frac{1}{2}$. Thus, the quadratic form for the Laplacian matrix Q reads

$$x^T Qx \geqslant kp + x_1^T Q_1 x_1 + x_2^T Q_2 x_2 - \sigma_1.$$

At the transition point p^*, we have

$$2kp^* \geqslant \min(\mu_{n-1}(Q_1),\ \mu_{n-1}(Q_2))\big(x_1^T x_1 + x_2^T x_2\big).$$

With $(x_1^T x_1 + x_2^T x_2) = 1$, the transition threshold p^* is lower bounded by

$$p^* \geqslant \frac{\min(\mu_{n-1}(Q_1),\ \mu_{n-1}(Q_2))}{2k}. \tag{10}$$

Figure 2 shows the accuracy of the upper (9) and lower (10) bounds for interdependent networks of size $N = 1000$ that consist of two Erdős-Rényi graphs, panel (a) as well as two Barabási-Albert graphs, panel (b), with average degree $d_{av} = 6$. The interconnection pattern is a 2-to-2 ($k = 2$) scheme. As can be seen in the figure, the upper bound is more accurate for the two ER networks, whereas the lower bound seems to work slightly better the other way around. We also note that in [10], it was shown that the transition threshold p^* is upper bounded by $p^* \leqslant \frac{1}{4}\mu_{N-1}(Q_1 + Q_2)$ when $B = pI$ (the k-to-k interconnection with $k = 1$). For this case, the exact value of p^* was determined in [12], however, the method used cannot be readily generalized to a 2-to-2 nor to a general k-to-k ($k \geqslant 2$) interconnection pattern.

B. Exact expression using the quotient graph

In this subsection, we present an analytical approach to calculate the exact transition threshold for a class of networks. The approach uses partitions of graphs in each layer and the corresponding quotient graph [28] whose transition threshold is analytically solvable.

Let us first focus on the partitions of the graph in each layer. For a k-to-k interconnection pattern, we assume the graph G_1 of n nodes consists of $\frac{n}{k}$ subgraphs $H_1^{(1)}, \dots, H_{n/k}^{(1)}$ where each subgraph has exactly k nodes and $\frac{n}{k}$ is an integer. In other words, k is chosen in such a way that $k \mid n$, i.e., k is a divisor of n. Analogously, a similar form is assumed for graph G_2, resulting in the subgraphs $H_1^{(2)}, \dots, H_{n/k}^{(2)}$. Without loss of generality, we demonstrate the whole approach by using graph G_1 and denote $\frac{n}{k}$ by m. After the division, subgraphs H_i are ordered as a chain and each subgraph connects to its neighboring subgraphs. The adjacency matrix A_1 of graph G_1, consisting of divided subgraphs H_i and connected as a chain, can be written as a block matrix

$$A_1 = \begin{bmatrix} A_{H_1} & R_1 & & \\ R_1^T & A_{H_2} & R_2 & \\ & \ddots & \ddots & \ddots \\ & & R_m^T & A_{H_m} \end{bmatrix}, \tag{11}$$

where the $k \times k$ adjacency matrix for a subgraph H_i is denoted by A_{H_i}.

In order to calculate the exact transition threshold, we perform a coarse-grained process by condensing each subgraph H_i into a node and two nodes are connected if two subgraphs are connected. The resulting graph corresponding to the partition is also called the quotient graph [28]. The link between nodes i and j in the quotient graph is weighted by the average degree $\widetilde{d_{ij}}$ that a node in subgraph H_i has in subgraph H_j. The adjacency matrix of the quotient graph of G_1 reads

$$(\widetilde{A_1})_{m\times m} = \begin{bmatrix} \widetilde{d_{11}} & \widetilde{d_{12}} & & \\ \widetilde{d_{21}} & \widetilde{d_{22}} & \widetilde{d_{23}} & \\ & \ddots & \ddots & \ddots \\ & & \widetilde{d_{m,m-1}} & \widetilde{d_{mm}} \end{bmatrix}.$$

If the k-to-k interconnection is attained by fully connecting subgraph $H_i^{(1)}$ in graph G_1 to the subgraph $H_i^{(2)}$ in graph G_2, then the Laplacian of the quotient graph of the whole interdependent network is

$$\widetilde{Q} = \begin{bmatrix} (\widetilde{Q_1})_{m\times m} + kpI & -kpI \\ -kpI & (\widetilde{Q_2})_{m\times m} + kpI \end{bmatrix}, \tag{12}$$

where

$$(\widetilde{Q_1})_{ij} = \begin{cases} -\widetilde{d_{ij}} & \text{if } \; i \neq j \\ \sum_{s=1, s\neq i}^{m} \widetilde{d_{is}} & \text{if } \; i = j \end{cases}.$$

When the quotient Laplacian preserves the algebraic connectivity of the original graph, then by applying the method proposed in [12] to the quotient Laplacian (12), the transition

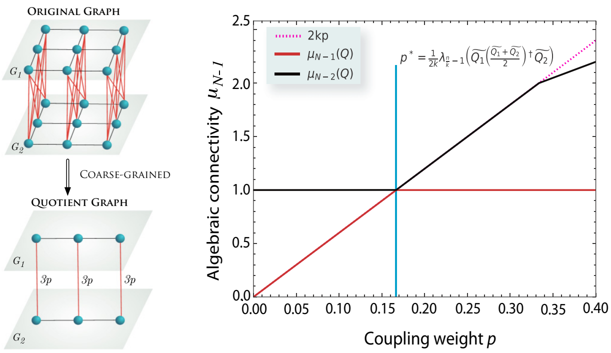

FIG. 3. Example topology with k-to-k ($k = 3$) interconnections whose transition threshold is calculated exactly by (13).

occurs at

$$p^* = \frac{1}{2k}\lambda_{m-1}\left[\widetilde{Q_1}\left(\frac{\widetilde{Q_1}+\widetilde{Q_2}}{2}\right)^{\dagger}\widetilde{Q_2}\right], \tag{13}$$

where $\dagger$ denotes the pseudoinverse [29] and λ_{m-1} denotes the second smallest eigenvalue. Figure 3 shows an example for which the transition threshold is determined by (13).

Next, we construct a class of graphs whose algebraic connectivity is preserved in the corresponding quotient graphs. The Cartesian product $\hat{G}_1 \Box \hat{G}_2$ of two graphs $\hat{G}_1$ and $\hat{G}_2$ with node set $\mathcal{N}_1$ and $\mathcal{N}_2$ is a graph such that (i) the node set of $\hat{G}_1 \Box \hat{G}_2$ is $\mathcal{N}_1 \times \mathcal{N}_2$ and (ii) two nodes $i_1 i_2$ and $j_1 j_2$ are connected in $\hat{G}_1 \Box \hat{G}_2$ if either $i_1 = j_1$ and i_2 is connected to j_2 or $i_2 = j_2$ and i_1 is connected to j_1. If all the subgraphs in (11) are identical and the matrix R is the identity matrix, the two-layer coupled network can be written as the Cartesian product of the subgraph $H_1^{(1)}$ fully connected with subgraph $H_1^{(2)}$ and the path graph P_m with $m = \frac{n}{k}$ nodes. The corresponding quotient graph can be obtained by the Cartesian product of a path graph with 2 (number of layers) nodes weighted by kp and a path graph with m nodes. The adjacency matrix of the original graph and the quotient graph thus follows

$$A = \begin{bmatrix} A_{H_1^{(1)}} & pJ_{k\times k} \\ pJ_{k\times k} & A_{H_1^{(2)}} \end{bmatrix} \Box \, A_{P_m} \tag{14}$$

and

$$\widetilde{A} = \begin{bmatrix} 0 & kp \\ kp & 0 \end{bmatrix} \Box \, A_{P_m}, \tag{15}$$

where $\Box$ represents the Cartesian product. The example topology in Fig. 3 can be obtained from the Cartesian product as shown in Fig. 4.

If two graphs G_1 and G_2 have Laplacian eigenvalues $\mu(G_1)$ and $\mu(G_2)$, then the Laplacian eigenvalues of the Cartesian product [30] of G_1 and G_2 are $\mu(G_1) + \mu(G_2)$. Thus, the Laplacian eigenvalues of the quotient graph are those of the path graph P_m plus those of P_2 with weight kp. The second smallest eigenvalue can be either $2kp$ of the path P_2 or $\mu_{m-1}(P_m)$ of the path P_m. Similarly, the Laplacian

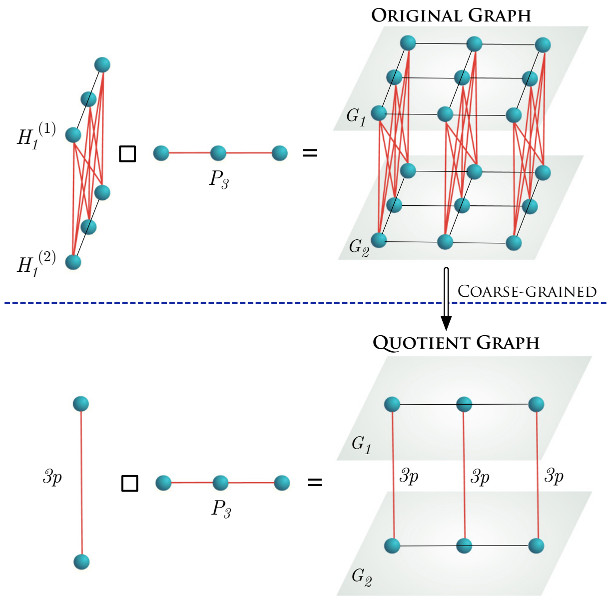

FIG. 4. The figure illustrates how the example topology in Fig. 3 can be obtained from the Cartesian product of subgraphs.

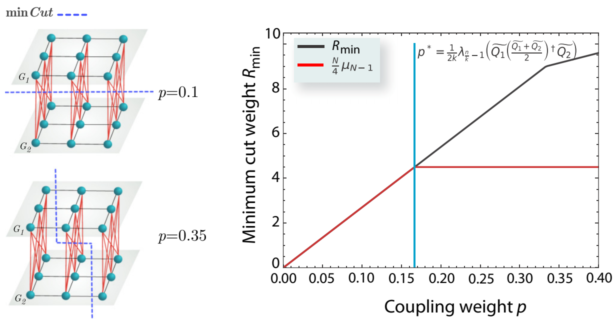

FIG. 5. When $p \leqslant p^*$, the minimum cut is achieved by cutting all the interdependent links and the minimized cut weight follows $R_{\min} = \frac{N}{4}\mu_{N-1}$.

eigenvalues of the original graph are those of path graph P_m plus those of the fully connected subgraphs $H_1^{(1)}$ and $H_1^{(2)}$. The second smallest eigenvalue can be either $2kp$ of the fully connected $H_1^{(1)}$ and $H_1^{(2)}$ or $\mu_{m-1}(P_m)$ of the path P_m. For this particular class of graphs, the quotient graph preserves the algebraic connectivity, which follows $\min\{2kp,\ \mu_{m-1}(P_m)\}$, of the original graph. The approach can be applied to the coarse graining of these particular graphs such that certain Laplacian eigenvalues are preserved, which is arguably a key issue to analyze for large complex networks [31,32]. Moreover, Cozzo and Moreno [33] employed coarse-grained or quotient graphs to characterize multiple structural transitions of coupled (with $k = 1$) multilayer networks.

IV. PHYSICAL MEANING OF p^* IN TERMS OF THE MINIMUM CUT

In graph theory, a cut [21] is defined as the partition of a graph into two disjoint subgraphs $\widetilde{G}_1$ and $\widetilde{G}_2$. A cut set refers to a set of links between subgraphs $\widetilde{G}_1$ and $\widetilde{G}_2$. For a weighted graph, the minimum cut refers to a cut set whose cut weight R is minimized, where the cut weight R is the sum of link weights over all links in the cut set. In this paper, we consider interdependent networks G that are weighted, where each link within graphs G_1 and G_2 has weight 1 and each link between graphs G_1 and G_2 has weight p.

A normalized index vector y for a cut of a graph G into subgraphs $\widetilde{G}_1$ and $\widetilde{G}_2$ is defined as

$$y_i = \sqrt{\frac{1}{N}} \begin{cases} 1 & \text{if node } i \in \widetilde{G}_1 \\ -1 & \text{if node } i \in \widetilde{G}_2 \end{cases},$$

where $y^T y = 1$. The cut weight R follows [21] from the quadratic form of the Laplacian matrix Q

$$R = \frac{N}{4}\left(\sum_{l \in \mathcal{L}^{\text{intra}}} (y_{l^+} - y_{l^-})^2 + p \sum_{l \in \mathcal{L}^{\text{inter}}} (y_{l^+} - y_{l^-})^2 \right)$$
$$= \frac{N}{4} y^T Q y,$$

where $\mathcal{L}^{\text{intra}}$ and $\mathcal{L}^{\text{inter}}$ denote the set of links within layers and between different layers, respectively. There is a factor of $\frac{N}{4}$ because $|y_{l^+} - y_{l^-}| = \frac{2}{\sqrt{N}}$ if the starting node l^+ and the ending node l^- of a link l belong to different subgraphs, otherwise $y_{l^+} - y_{l^-} = 0$. The minimum cut is [21]

$$R_{\min} = \frac{N}{4} \min_{y \in \mathbb{Y}} y^T Q y,$$

where $\mathbb{Y}$ is the set of all possible normalized index vectors of the N-dimensional space. Rayleigh's theorem [21] states that, for any normalized vector y orthogonal to the all-one vector u, we have that $\mu_{N-1} \leqslant \frac{y^T Q y}{y^T y} \leqslant y^T Q y$ because $y^T y = 1$, and the equality holds when y is an eigenvector associated to μ_{N-1}. With $\mu_{N-1} \leqslant y^T Q y$, the minimum cut $R_{\min}$ follows

$$R_{\min} \geqslant \frac{N}{4}\mu_{N-1}.$$

If the index vector y is an eigenvector of G associated to the eigenvalue μ_{N-1}, then we obtain that $R_{\min} = \frac{N\mu_{N-1}}{4}$. On the other hand, Corollary 1 implies that the eigenvalue $\mu^* = 2kp$ can be made the second smallest eigenvalue μ_{N-1} with eigenvector $x = \frac{1}{\sqrt{N}}[u_n^T,\ -u_n^T]^T$ if $p < p^*$. In this regime, the partition corresponding to $y = x$ results in the minimum cut with $R_{\min} = \frac{N\mu_{N-1}}{4}$. The resulting subgraphs from that partition are exactly graphs G_1 and G_2 and the cut set contains all the interdependent links. Contrarily, when the coupling weight $p > p^*$, the eigenvector $x = \frac{1}{\sqrt{N}}[u_n^T,\ -u_n^T]^T$ is no longer an eigenvector of graph G associated to the second smallest eigenvalue μ_{N-1} and, therefore, cutting all the interdependent links is not guaranteed to be the minimum cut. Figure 5 shows the minimum cut before and after the phase transition p^* using the same example as Fig. 3.

In summary, the physical meaning of p^* in terms of the minimum cut is that if $p < p^*$, the minimum cut can be obtained by cutting all the interdependent links and the minimum cut weight follows $R_{\min} = \frac{N}{4}\mu_{N-1}$, whereas above the transition point, i.e., when $p > p^*$, the minimum cut involves both links within each subgraph and interdependent edges between the two subgraphs of the interdependent network G and the minimum cut weight is lower bounded by $\frac{N}{4}\mu_{N-1}$.

V. EXACT THRESHOLD FOR SPECIAL STRUCTURES OF INTERDEPENDENT NETWORKS

In this section, we analytically determine the structural threshold p^* for special graphs G_1 and G_2 or a special interconnection matrix B.

A. Coupled identical circulant graphs

Let x_{n-1} be the eigenvector associated to the second smallest eigenvalue $\mu_{n-1}(Q_1)$ of the Laplacian matrix Q_1 of graph G_1. For vector $x = (x_{n-1}^T,\ x_{n-1}^T)^T$ and $Q_2 = Q_1$, the eigenvalue equation in (2) reads

$$\begin{bmatrix} Q_1 + kpI & -p\hat{B} \\ -p\hat{B}^T & Q_1 + kpI \end{bmatrix}\begin{bmatrix} x_{n-1} \\ x_{n-1} \end{bmatrix} = \begin{bmatrix} \mu_{n-1}(Q_1)x_{n-1} + kpx_{n-1} - p\hat{B}x_{n-1} \\ \mu_{n-1}(Q_1)x_{n-1} + kpx_{n-1} - p\hat{B}^T x_{n-1} \end{bmatrix}, \quad (16)$$

where $\hat{B}$ is a zero-one matrix satisfying $\hat{B} = \frac{B}{p}$. As mentioned in Sec. II, circulant matrices are commutative. If two matrices commute, the two matrices have the same set of eigenvectors [21]. When Q_1 and $\hat{B}$ are symmetric circulant matrices, Q_1 and $\hat{B}$ commute, i.e., $Q_1\hat{B} = \hat{B}Q_1$, and the eigenvectors of Q_1 and $\hat{B}$ are the same [21]. The eigenvector x_{n-1} of the Laplacian Q_1 is also an eigenvector of matrix $\hat{B}$ belonging to the eigenvalue λ, where $\lambda = \frac{x_{n-1}^T\hat{B}x_{n-1}}{x_{n-1}^T x_{n-1}} = 2x_{n-1}^T\hat{B}x_{n-1}$ because the normalization $x^T x = 2x_{n-1}^T x_{n-1} = 1$. Substituting $\hat{B}x_{n-1} = \lambda x_{n-1}$ in (16) yields

$$\begin{bmatrix} Q_1 + kpI & -p\hat{B} \\ -p\hat{B}^T & Q_1 + kpI \end{bmatrix}\begin{bmatrix} x_{n-1} \\ x_{n-1} \end{bmatrix} = [mu_{n-1}(Q_1) + kp - \lambda p]\begin{bmatrix} x_{n-1} \\ x_{n-1} \end{bmatrix}.$$

The vector $x = (x_{n-1}^T,\ x_{n-1}^T)^T$ is an eigenvector of Q associated to eigenvalue $\mu = \mu_{n-1}(Q_1) + (k - \lambda)p$.

When the coupling weight p is small enough, the nontrivial eigenvalue $\mu^* = 2kp$ in (4) can be the algebraic connectivity μ_{N-1} and the eigenvalue $\mu_{n-1}(Q_1) + (k - \lambda)p$ can be made to be the third smallest eigenvalue μ_{N-2}. As already pointed out before, by increasing the coupling weight p, a transition of the algebraic connectivity μ_{N-1} occurs, where $\mu^* = 2kp$ is no longer the second smallest one. As the transition occurs at the point p^* such that $2kp^* = \mu_{n-1}(Q_1) + (k - \lambda)p^*$, one gets

$$p^* = \frac{\mu_{n-1}}{k + \lambda},$$

where $\lambda = 2x_{n-1}^T\hat{B}x_{n-1}$.

Figure 6(a) shows the algebraic connectivity of an interdependent network that consists of two identical circulant graphs with a 2-to-2 ($k = 2$) interconnection. The size of each circulant graph is $n = 100$ with average degree $d_{av} = 6$. When the coupling strength $p \leqslant p^*$, the algebraic connectivity μ_{N-1} is $4p$. When $p \geqslant p^*$, the algebraic connectivity in Fig. 6(a) is analytically expressed as $\mu_{N-1} = \mu_{n-1}(Q_1) + (2 - \lambda)p$. The transition occurs at the point $p^* = \frac{\mu_{n-1}}{2+\lambda}$, where $\lambda = 2x_{n-1}^T\hat{B}x_{n-1}$.

B. n-to-n interconnection

For an n-to-n interconnection pattern, the Laplacian matrix of the interdependent graph G reads

$$Q = \begin{bmatrix} Q_1 + pnI & -pJ_{n\times n} \\ -pJ_{n\times n} & Q_2 + pnI \end{bmatrix},$$

where the $n \times n$ all-one matrix J represents that one node in graph G_1 connects to all nodes in graph G_2 and vice versa. Graph G is the join [34] of graphs G_1 and G_2 if the coupling weight $p = 1$.

Let x_1 be the eigenvector associated to the eigenvalue $\mu_{n-1}(Q_1)$ of graph G_1 and x_2 be the eigenvector associated to the eigenvalue $\mu_{n-1}(Q_2)$ of graph G_2. For vectors $x = (x_1^T,\ 0)^T$ and $x = (0,\ x_2^T)^T$, the eigenvalue equation for the Laplacian matrix Q of G can be written as

$$\begin{bmatrix} Q_1 + pnI & -pJ \\ -pJ & Q_2 + pnI \end{bmatrix}\begin{bmatrix} x_1 \\ 0 \end{bmatrix} = [\mu_{n-1}(Q_1) + np]\begin{bmatrix} x_1 \\ 0 \end{bmatrix},$$

$$\begin{bmatrix} Q_1 + pnI & -pJ \\ -pJ & Q_2 + pnI \end{bmatrix}\begin{bmatrix} 0 \\ x_2 \end{bmatrix} = [\mu_{n-1}(Q_2) + np]\begin{bmatrix} 0 \\ x_2 \end{bmatrix}.$$

Similarly to the previous derivation, also for an n-to-n ($k = n$) interconnection, the nontrivial eigenvalue $\mu^* = 2np$ can be made equal to the algebraic connectivity $\mu_{N-1}(Q)$ of the Laplacian Q if the coupling weight p is small. Moreover, the eigenvalue $\min\{\mu_{n-1}(Q_1),\ \mu_{n-1}(Q_2)\} + np$ can be the third smallest eigenvalue $\mu_{N-2}(Q)$ for small values of p. Taking into account that the transition threshold p^* occurs when $\mu_{N-1}(Q) = \mu_{N-2}(Q)$, we get

$$p* = \min\left\{\frac{\mu_{n-1}(Q_1)}{n},\ \frac{\mu_{n-1}(Q_2)}{n}\right\}. \quad (17)$$

Figure 6(b) shows the algebraic connectivity of the interdependent network consisting of two Erdős-Rényi graphs $G_p(n)$ with $n = 500$ nodes and average degree $d_{av} = 6$. The interconnection pattern in this figure is n to n. Figure 6(b) demonstrates that when the coupling weight p is small, the algebraic connectivity is $\mu_{N-1} = 2np$. With the increase of p, the algebraic connectivity is described by $\mu_{N-1} = \min\{\mu_{n-1}(Q_1),\ \mu_{n-1}(Q_2)\} + np$. The transition occurs when $2np = \min\{\mu_{n-1}(Q_1),\ \mu_{n-1}(Q_2)\} + np$ and the threshold p^* obeys (17).

C. $(n-1)$-to-$(n-1)$ interconnection

When $B = p(J - I)$ and $G_2 = G_1$, the eigenvalue equation for the Laplacian matrix Q reads, with vector $x =$

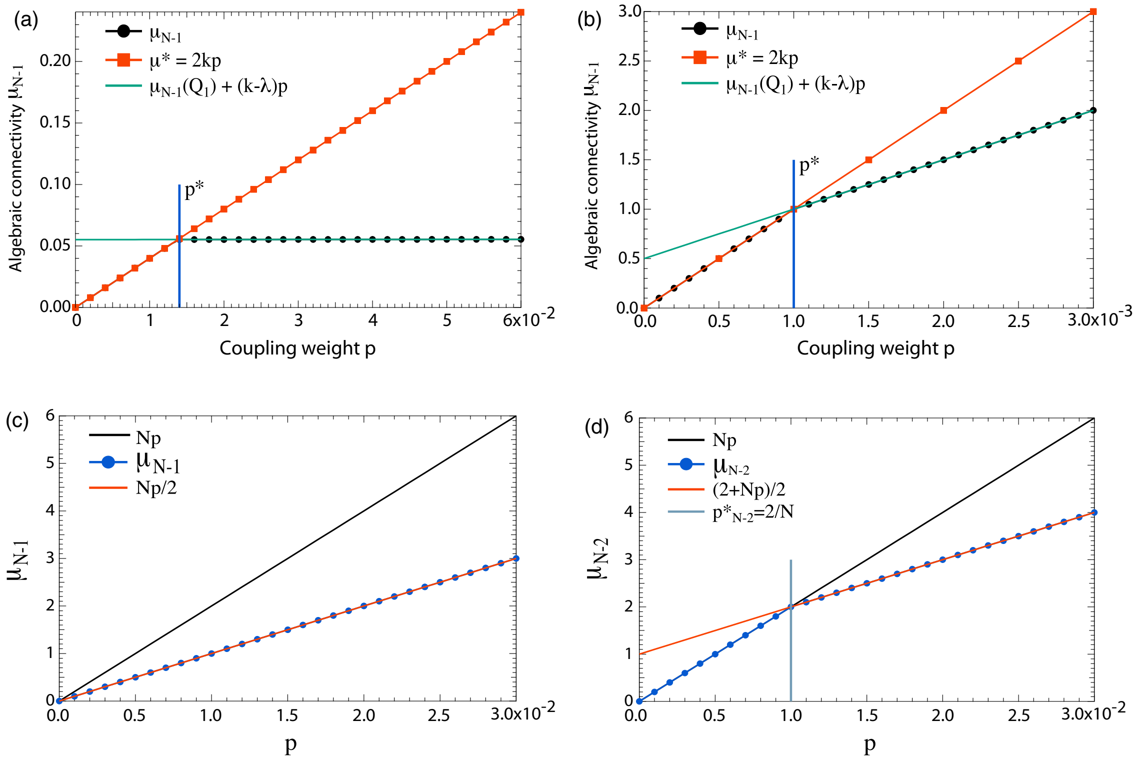

FIG. 6. Exact transition threshold for special structures including (a) coupled circulant graphs, (b) fully coupled Erdős-Rényi graphs, and (c),(d) a star graph fully coupled with its complementary graph.

$(x_{n-1}^T, -x_{n-1}^T)^T$ where x_{n-1} is an eigenvector associated to the algebraic connectivity $\mu_{n-1}(Q_1)$ of graph G_1, as

$$\begin{bmatrix} Q_1 + p(n-1)I & -p(J-I) \\ -p(J-I) & Q_1 + p(n-1)I \end{bmatrix} \begin{bmatrix} x_{n-1} \\ -x_{n-1} \end{bmatrix} = [\mu_{n-1}(Q_1) + (n-2)p] \begin{bmatrix} x_{n-1} \\ -x_{n-1} \end{bmatrix}. \quad (18)$$

The nontrivial eigenvalue follows $\mu^* = 2(n-1)p$ for an $(n-1)$-to-$(n-1)$ interconnection. When p is small, the eigenvalue $2(n-1)p$ can be made equal to μ_{N-1} and the eigenvalue $\mu_{n-1}(Q_1) + (n-2)p$ can be the third smallest eigenvalue μ_{N-2}. At the transition $p = p^*$, we have that $\mu_{N-1} = \mu_{N-2}$ from which the threshold p^* follows as

$$p* = \frac{\mu_{n-1}(Q_1)}{n}.$$

D. A graph coupled with its complementary graph

The complementary graph G_1^c of a graph G_1 has the same set of nodes as G_1 and two nodes are connected in G_1^c if they are not connected in G_1 and vice versa [21]. The adjacency matrix of the complementary graph G_1^c is $A_1^c = J - I - A_1$. The Laplacian of the complementary graph G_1^c follows $nI - J - Q_1$.

For an interdependent graph G consisting of a graph G_1 and its complementary graph G_1^c with an n-to-n interconnection pattern, the Laplacian matrix Q of the interdependent graph G reads

$$Q = \begin{bmatrix} Q_1 + npI & -pJ \\ -pJ & nI - J - Q_1 + npI \end{bmatrix}.$$

Let x_{n-1} be the eigenvector associated to the eigenvalue μ_{n-1} of the graph G_1 and x_1 be the eigenvector associated to the eigenvalue μ_1. For vectors $x = (x_{n-1}^T, 0)^T$ and $x = (0, x_1^T)^T$, the eigenvalue equation for the Laplacian matrix Q of G can be written as

$$\begin{bmatrix} Q_1 + npI & -pJ \\ -pJ & nI - J - Q_1 + npI \end{bmatrix} \begin{bmatrix} x_{n-1} \\ 0 \end{bmatrix} = [\mu_{n-1}(Q_1) + np] \begin{bmatrix} x_{n-1} \\ 0 \end{bmatrix}, \quad (19)$$

$$\begin{bmatrix} Q_1 + npI & -pJ \\ -pJ & nI - J - Q_1 + npI \end{bmatrix} \begin{bmatrix} 0 \\ x_1 \end{bmatrix} = [n + np - \mu_1(Q_1)] \begin{bmatrix} 0 \\ x_1 \end{bmatrix}. \quad (20)$$

Following the same procedure as in the previous examples, at the transition point we have that the equality $\mu_{N-1}(Q) = \mu_{N-2}(Q)$ holds, which yields

$$p* = \min\left(\frac{\mu_{n-1}(Q_1)}{n}, 1 - \frac{\mu_1(Q_1)}{n}\right).$$

E. An example of the nonexistence of the structural transition

In this subsection, we consider an interdependent network consisting of a star graph G_1 and its complementary graph G_1^c while the interconnection pattern is n to n. For a star graph with size n, the eigenvalues of the Laplacian [21] are 0, 1 with multiplicity $n-2$ and n. Substituting $\mu_{n-1}(Q_1)=1$ and $\mu_1(Q_1)=n$ into eigenvalue equations (19) and (20) yields two eigenvalues np and $np+1$.

When the coupling weight $p>0$, the nontrivial eigenvalue $\mu^*=2np$ cannot be the second smallest eigenvalue of the Laplacian Q because it is always larger than the eigenvalue np. Hence, the transition between μ^* and the algebraic connectivity $\mu_{N-1}(Q)$ will never occur as shown in Fig. 6(c). Nonexistence of such transition in multiplex networks of one-to-one interconnection is also reported when at least one of the two layers has vanishing algebraic connectivity [12]. Instead, when p is small, the nontrivial eigenvalue $\mu^*=2np$ can be made the third smallest eigenvalue $\mu_{N-2}(Q)$. By increasing the coupling weight p, the eigenvalue $\mu^*=2np$ may no longer be the third smallest eigenvalue of the Laplacian Q. There exists a threshold denoted as p^*_{N-2} such that $\mu^*=2np$ exceeds $\mu_{N-2}(Q)$ when $p>p^*_{N-2}$. When $p\leqslant p^*_{N-2}$ then the third smallest eigenvalue follows $\mu_{N-2}(Q)=2np$. Above the transition point p^*_{N-2}, the nontrivial eigenvalue $\mu^*=2np$ exceeds eigenvalue $1+np$. The transition occurs when $2np*=1+np*$ resulting in $p^*_{N-2}=\frac{1}{n}$. Figure 6(d) shows that the transition occurs at the point $p^*_{N-2}=\frac{1}{n}$.

Note, however, that in the above example, the complementary graph G_1^c of a star is a disconnected graph. The hub node in the star G_1 is an isolated node in graph G_1^c. The coupling is stronger between graph G_1 and the connected component in graph G_1^c than that between graph G_1 and the isolated node in G_1^c. The isolated node first decouples from the interdependent network G before the connected component in G_1^c decouples from the interdependent graph G. As a result, the structural transition in p occurs at the third smallest eigenvalue rather than at the second smallest eigenvalue. The above example also agrees with the upper bound in (9) in that the threshold $p^*=0$ when $\mu_{n-1}(Q_1)=0$ or $\mu_{n-1}(Q_2)=0$. There is no transition between the nontrivial eigenvalue $\mu^*=2kp$ and the algebraic connectivity μ_{N-1}, if one of the coupled graphs is disconnected.

VI. CONCLUSION

In this paper, we have studied the structural transition of interdependent networks. We first generalized the one-to-one interconnection coupling to a general k-to-k intercoupling scheme for interdependent networks. This representation of the couplings between the networks that made up the whole system is more realistic and could represent more situations of practical interest. However, we acknowledge that the interconnection matrix B representing the k-to-k interconnection obeys regularity (constant row and column sum), which still represents a simplification of real systems. Nonetheless, the more complex scenario addressed here allows us to deduce the nontrivial eigenvalue of such interdependent networks [1].

For the general k-to-k interconnection ($B\neq pI$ unless $k=1$) studied throughout this paper, a number of results and properties of the transition threshold p^* can be readily obtained. For connected graphs G_1 and G_2, we showed that the transition threshold p^* is upper bounded by the minimum algebraic connectivity of graphs G_1 and G_2 divided by k. Additionally, we have shown that networks that are divisible to regularly interconnected subgraphs show a transition threshold that is determined from the coarse-grained or quotient graph. These results could be important in some applications. For instance, the bounds and the exact value of the transition threshold p^* can be used to identify the interactions and the multilayer coupling pattern of neural networks, as they have been suggested to operate, in a healthy human brain, around the transition point [17]. Our physical interpretation of the threshold p^* is also of interest. Namely, we have argued that below the transition threshold p^*, the minimum cut of the network includes all the interconnection links, whereas above it, the minimum cut might contain both the interconnection links between graphs G_1 and G_2 and the links within G_1 and G_2. Finally, we have derived exact expressions for the threshold p^* for some special topologies, and shown that if one of the graphs G_1 or G_2 is disconnected, then the structural threshold p^* for the algebraic connectivity does not exist. Altogether, our results allow further advances into the theory of multilayer networks and could pave the way to similar studies that consider more realistic networks.

ACKNOWLEDGMENTS

We are very grateful to C. Scoglio for valuable discussions. This research was supported by the China Scholarship Council (CSC). Y.M. acknowledges partial support from the Government of Aragón, Spain through Grant No. E36-17R, and by MINECO and FEDER funds (Grant No. FIS2017-87519-P).

[1] P. Van Mieghem, Interconnectivity structure of a general interdependent network, Phys. Rev. E **93**, 042305 (2016).
[2] V. Rosato, L. Issacharoff, F. Tiriticco, S. Meloni, S. Porcellinis, and R. Setola, Modelling interdependent infrastructures using interacting dynamical models, Int. J. Crit. Infrastruct. **4**, 63 (2008).
[3] A. Vespignani, Complex networks: The fragility of interdependency, Nature (London) **464**, 984 (2010).
[4] R. Little, A socio-technical systems approach to understanding and enhancing the reliability of interdependent infrastructure systems, Int. J. Emerg. Manage. **2**, 98 (2004).
[5] S. V. Buldyrev, R. Parshani, G. Paul, H. E. Stanley, and S. Havlin, Catastrophic cascade of failures in interdependent networks, Nature (London) **464**, 1025 (2010).
[6] H. Wang, Q. Li, G. D'Agostino, S. Havlin, H. E. Stanley, and P. Van Mieghem, Effect of the interconnected network structure on the epidemic threshold, Phys. Rev. E **88**, 022801 (2013).
[7] E. Cozzo, R. A. Baños, S. Meloni, and Y. Moreno, Contact-based social contagion in multiplex networks, Phys. Rev. E **88**, 050801 (2013).
[8] S. Bonaccorsi, S. Ottaviano, F. De Pellegrini, A. Socievole, and P. Van Mieghem, Epidemic outbreaks in two-scale

community networks, Phys. Rev. E **90**, 012810 (2014).
[9] G. Ferraz de Arruda, E. Cozzo, T. P. Peixoto, F. A. Rodrigues, and Y. Moreno, Disease Localization in Multilayer Networks, Phys. Rev. X **7**, 011014 (2017).
[10] F. Radicchi and A. Arenas, Abrupt transition in the structural formation of interconnected networks, Nat. Phys. **9**, 717 (2013).
[11] J. Martín-Hernández, H. Wang, P. Van Mieghem, and G. D'Agostino, Algebraic connectivity of interdependent networks, Physica A (Amsterdam) **404**, 92 (2014).
[12] F. D. Sahneh, C. Scoglio, and P. Van Mieghem, Exact coupling threshold for structural transition reveals diversified behaviors in interconnected networks, Phys. Rev. E **92**, 040801 (2015).
[13] G. Rapisardi, A. Arenas, G. Caldarelli, and G. Cimini, Multiple structural transitions in interacting networks, Phys. Rev. E **98**, 012302 (2018).
[14] D. Ganesan, R. Cristescu, and B. Beferull-Lozano, Power-efficient sensor placement and transmission structure for data gathering under distortion constraints, ACM Trans. Sens. Networks **2**, 155 (2006).
[15] V. K. Sood, D. Fischer, J. Eklund, and T. Brown, Developing a communication infrastructure for the smart grid, in *Electrical Power & Energy Conference (EPEC)* (IEEE, Montreal, 2009), pp. 1–7.
[16] M. Parandehgheibi and E. Modiano, Robustness of interdependent networks: The case of communication networks and the power grid, in *2013 IEEE Global Communications Conference (GLOBECOM)* (IEEE, Atlanta, 2013), pp. 2164–2169.
[17] P. Tewarie, A. Hillebrand, B. W. van Dijk, C. J. Stam, G. C. O'Neill, P. Van Mieghem, J. M. Meier, M. W. Woolrich, P. G. Morris, and M. J. Brookes, Integrating cross-frequency and within band functional networks in resting-state MEG: A multi-layer network approach, Neuroimage **142**, 324 (2016).
[18] S. M. Rinaldi, J. P. Peerenboom, and T. K. Kelly, Identifying, understanding, and analyzing critical infrastructure interdependencies, IEEE Control Syst. **21**, 11 (2001).
[19] X. Wang, R. E. Kooij, and P. Van Mieghem, Modeling region-based interconnection for interdependent networks, Phys. Rev. E **94**, 042315 (2016).
[20] M. Kivelä, A. Arenas, M. Barthelemy, J. P. Gleeson, Y. Moreno, and M. A. Porter, Multilayer networks, J. Complex Networks **2**, 203 (2014).
[21] P. Van Mieghem, *Graph Spectra for Complex Networks* (Cambridge University Press, Cambridge, UK, 2011).
[22] A. Sandryhaila and J. M. Moura, Discrete signal processing on graphs, IEEE Trans. Signal Process. **61**, 1644 (2013).
[23] P. J. Davis, *Circulant Matrices* (American Mathematical Society, Providence, 2012).
[24] M. Fiedler, Algebraic connectivity of graphs, Czech. Math. J. **23**, 298 (1973).
[25] S. Gomez, A. Diaz-Guilera, J. Gomez-Gardeñes, C. J. Perez-Vicente, Y. Moreno, and A. Arenas, Diffusion Dynamics on Multiplex Networks, Phys. Rev. Lett. **110**, 028701 (2013).
[26] C. W. Wu, Synchronization in arrays of coupled nonlinear systems with delay and nonreciprocal time-varying coupling, IEEE Trans. Circuit Syst. II: Express Briefs **52**, 282 (2005).
[27] A. Jamakovic and P. Van Mieghem, On the robustness of complex networks by using the algebraic connectivity, in *International Conference on Research in Networking* (Springer, Berlin, 2008).
[28] R. Sánchez-Garcia, E. Cozzo, and Y. Moreno, Dimensionality reduction and spectral properties of multilayer networks, Phys. Rev. E **89**, 052815 (2014).
[29] P. Van Mieghem, K. Devriendt, and H. Cetinay, Pseudoinverse of the Laplacian and best spreader node in a network, Phys. Rev. E **96**, 032311 (2017).
[30] A. E. Brouwer and W. H. Haemers, *Spectra of Graphs* (Springer, New York, 2011).
[31] D. Gfeller and P. De Los Rios, Spectral Coarse Graining of Complex Networks, Phys. Rev. Lett. **99**, 038701 (2007).
[32] M. Faccin, M. T. Schaub, and J.-C. Delvenne, Entrograms and coarse graining of dynamics on complex networks, J. Complex Networks **6**, 661 (2017).
[33] E. Cozzo and Y. Moreno, Characterization of multiple topological scales in multiplex networks through supra-Laplacian eigengaps, Phys. Rev. E **94**, 052318 (2016).
[34] F. Harary, *Graph Theory* (Addision-Wesley, New Delhi, 1969).